ASM Sci. J.Special Issue 2018(1) AiMS2018, 86-95

Bimetallic PMMA@Alloy (Au-Ag) in 3D hot spots as highly sensitive substrate for high performance surface-enhanced Raman scattering (SERS)

S. Kassim[1,2*], R. A. A. Tahrin[1], N. F. Rusdi[1] and N. A. Harun[1,2]

[1]*School of Fundamental Science, Universiti Malaysia Terengganu, 21030 Kuala Nerus, Terengganu, Malaysia.*

[2]*Advanced Nano Materials (ANoMa) Research Group, School of Fundamental Science, Universiti Malaysia Terengganu, 21030 Kuala Nerus, Terengganu, Malaysia.*

A feasible production of poly (methyl methacrylate)@alloy (gold-silver) core shell has been presented as candidate in enhanced detection of surface enhanced Raman scattering (SERS). Free emulsifier- emulsion synthesised PMMA sphere with average size of 419 nm in diameter were used as core material for incorporation of alloy nanoparticles (6 nm) resulting a core-shell structure. The fabrication of PMMA@alloy SERS substrate was successfully done via self-assembly thus the produced SERS substrate that comprise of unique optical properties combination arising from periodic core arrangement and plasmonic activity of alloy nanoparticles. Alloy is bimetallic nanoparticles in which the combination of silver (Ag) and gold (Au) present an absolutely improved light resistance as compared to single metal alone with great surface plasmon resonance. Morphology and elemental analysis was performed through scanning electron microscope (SEM) and the analysis showing species of both Au and Ag in single alloy nanoparticles. The alloy nanoparticles were also observed to homogenously coating the PMMA sphere. Surface plasmon resonance activity was maximum at 476 nm obtained from UV-Visible spectroscopy. High surface production was observed to have periodically arranged PMMA@alloy core -shell and potentially to be used as SERS substrate.

Keywords: poly(methyl methacrylate), surface plasmon resonance, alloy nanoparticles, bimetallic, surface-enhanced Raman scattering (SERS)

I. INTRODUCTION

Surface enhanced Raman scattering (SERS) is label free tools with high sensitivity and powerful spectroscopy techniques for the analysis of molecular fingerprint along with excellent substrate thus establishing SERS to be important ranging from environmental monitoring, food quality control, analytical chemistry, biomedical and disease detection [1]-[5]. Accordingly most attempts to improve SERS activity has been fo-

*Corresponding author:syara.kassim@umt.edu.my

cused on achieving high-performance SERS substrates by using noble metal mainly including Au, Ag and Cu [6]-[9]. However sensitive and large area of identification and detection of unknown sample remain as huge challenge due to several limitation factor of substrate. Insufficient hot spot resulting from small surface area lead to weak signal enhancement followed with low molecular affinity for metal surface. Photonic SERS substrate currently has an intense interest among researchers in which the fabrication is the main focus [10]-[14]. Several studies were proposing to assemble nanoparticles in periodic arrangement to exhibit photonic band gap (PBG) properties however the cost behind this production is a huge deal. Furthermore the substrate has a narrow active area and the stability remain under argumentation.

Remarkable point is that Ag NPs produces a sharp resonance however their weak resistance towards light or easily oxidise in nature brings Au as a great option among researcher. Despites of their stability and generally inert, Au NPs were also believed in biocompatibility and scope for surface chemistry however the plasmonic activity is not as strong as silver [15]-[18]. Originates from this situation bimetallic (Au-Ag) alloy nanoparticles were synthesised in this work to improve both physical and chemical properties compared to single metal nanoparticles. Polymer core material has been selected in most research due to its easily controlled size and shape [19]-[20]. Poly (methyl methacrylate) spheres were selected as core material according to its feasible production, tunable particles size, reproducible, and could be removed easily if using as template for further work [21]-[26]. Besides PMMA sphere could simultaneously stabilize metal nanoparticles from agglomerates by preparing a sites for the nanoparticles to homogenously incorporate. Upon fabricating, PMMA sphere obeyed to assemble in periodic manner thus exhibited photonic band gap (PBG) properties thus an idea of combining metal properties together with this photonic crystals could be enhanced the performance of SERS substrate threefold.

In this work, 3D metallodielectric photonic crystals SERS substrate was synthesized and fabricated to demonstrate as highly sensitive performance towards 4-aminothiolphenol. PMMA spheres were prepared via free-emulsifier emulsion polymerization continue with surface modification with polyethylene imine (PEI) [27]. Alloy nanoparticles were prepared by reducing the silver and gold precursor with sodium citrate and introduced to modified PMMA/PEI. 3D fabrication was done through bottom-up technique by self-assemble the SERS substrate and ready for SERS probe molecule casting. Morphology study was performed on both fabricated PMMA thin film and PMMA@alloy dispersion to observe the periodicity of the assembled sphere and homogeneity. The morphology of final SERS substrate and nanoparticles was observed and elemental mapping analysis

was done to investigate percentage of element species for Au, Ag and carbon (carbon represents PMMA). Surface plasmon resonance′s peak of alloy nanoparticles and the core-shell were compared and discussed in relation to the SERS activity.

II. EXPERIMENTAL PROCEDURE

A. Materials

Methyl methacrylate monomer (MMA, 99%), poly (sodium -4-styrenesulfonate) (PSSS), polyethylene imine (80% ethoxylated solution) (PEI) and gold (III) chloride hydrate (∼50% Au basis) ($HAuCl_4$) were purchased from Aldrich (Milwaukee, WI, USA), while potassium persulphate (KPS) and trisodium citrate (TSC) were purchased from RM Marketing (U.K). Silver nitrate ($AgNO_3$) was purchased from Bendosen Laboratory Chemicals and deionized water (resistivity 18.0 MΩ) was used for the preparation of all solutions. All chemicals and solvents were used as received without further purification. All reactions were carried out in the fume hood.

B. Synthesis PMMA@alloy coreshell

Monodispersed PMMA spheres with average size of 427 nm were initially synthesized via surfactant free emulsion polymerization [28]. Where 64 ml of deionized water, 10 ml monomers MMA and 16 ml of initiator KPS (0.13 M) were fed onto a tri-neck round-bottom flask equipped with a nitrogen inlet tube and water cooled reflux condenser. This polymerization was carried out by heating at 90 °C with an automatically controlled silicon oil bath and hotplate stabilizer rod. Milky white colloidal suspension was observed after 15 minutes and the reaction was continued for another 30 minutes for complete the polymerization. The obtained colloidal suspension (PMMA) was then filtered and continued with centrifugation (Eppendorf 5810, Germany) step at 3800 rpm for 25 minute to results homogenous PMMA spheres for further use.

PMMA was undergone surface modification by using PEI before incorporated with alloy NPs in which alloy nanoparticles were separately prepared by using citrate reducing agent. 78 ml of deionized water was boiled at 100 °C, while stirring at 300 rpm. 1ml of $AgNO_3$(1mM) and $HAuCl_4$ (1mM) were carefully dropped into the flask followed with addition of 8ml TSC (0.1M) immediately. The reaction was continued at 100°C and 300 rpm for 15 minutes. The resulting alloy NPs suspension was centrifuged and redispersed. The solution was let to cool at room temperature before incorporated onto PMMA/PEI spheres. PMMA/PEI suspension was dropped into alloy nanoparticles suspension and the reaction was stirred (450 rpm) for a day at room temperature to form the core-shell. PMMA@ alloy core-shell was centrifuged and redispersed for fabrication and characterization.

C. Fabrication

Fabrication of PMMA thin film and PMMA@ alloy CS (3D MDPC SERS) substrate was done via self-assembly technique. 1 cm x 2 cm size microscope glass slide was settled 45° in either PMMA or PMMA@ alloy suspension and let grow in an oven (Eppendorf, Germany) at 60 °C for 2 days.

D. Characterization

The average diameter and polydispersity of polymer particles dispersion were measured by using particle size analyzer (PSA, Malvern, UK) and dynamic light scattering (DLS, Malvern, UK) together with analysing the zeta potential of polymer and alloy NPs. The morphology of PMMA and PMMA@alloy CS was observed by using scanning electron microscopy (SEM, JEOL model 6360F) images and the composition of coreshell were confirmed by electron dispersive X-ray spectroscopy (EDS). A drop of dispersion and also thin film was placed on a sample stub and dried before SEM viewing. Alloy NPs and the core-shell was investigate it potentiality in photonic applications by using UV-Vis spectroscopy (Shimadzu, Japan).

III. RESULT AND CHARACTERIZATION

The average size and surface charge of the material in every stage of preparation is summarised in Table 1. Accordingly 427 nm poly (methyl methacrylate) (PMMA) spheres with polydispersity index (PDI) of 1.35% was obtained. From the PDI data, it can be concluded that the PMMA spheres have a low size dispersion thus homogenously in suspension. The homogeneity of core material which is PMMA is a key factor in achieving an excellent photonic band gap (PBG) properties in further fabrication as SERS substrate. Homogenous PMMA sphere would produce a high order sequence during fabrication thus resulting in photonic crystals with nearly complete PBG. Zeta potential (ζ-potential) is well known technique for determining the surface charge of nanoparticles in solution (colloids). Thus in this work, ζ-potential is another confirmation indicator besides to determine if a surface modification to the nanoparticle has been successful or if a processing step has modified the nanoparticle surface. High ζ-potential (usually in range of +25 mV and -25 mV) reveals high degree of long term stability of suspension while dispersions with a low ζ-potential value will eventually aggregate due to van der Waal inter-particle attractions. By relying on this PMMA spheres, alloy nanoparticles and the core-shell have low tendency to aggregates in long time period. Surface modification of PMMA with PEI was also successfully obtained by comparing the charge value of PMMA and PMMA /PEI is -31.36 mV and +48.86 mV respectively. Furthermore, the stability of dispersion after modification was also

notified. Alloy nanoparticles (Alloy NPs) however have problems in determining the actual value due to limitation of zeta size in which particles with diameters of <20 nm have a high mobility in solution due to the applied field and Brownian motion. In addition, these particles have very low light scattering properties thus satisfactory quality result hardly being analysed. However the surface charge of alloy NPs still could be finalised even with a very low value of ζ-potential thus linking PEI in between PMMA and alloy NPs is promoting the incorporation of alloy on PMMA surface. Average size of alloy NPs (6 nm) however was obtained from electron micrograph measurement tools with standard deviation of 0.02 (Figure 2 (c)).

Table 1. Average particle size and surface charge of PMMA, PMMA/PEI and alloy NPs.

Materials	Average size (nm)	PDI index (%)	Surface charge (mV)
PMMA	427	1.35	1.35
PMMA/PEI	-	-	+48.86
Alloy NPs	6 nm	-	-9.94

Physically, Figure 1 shows the obtained silver nanoparticles with golden orange colour indicating the existence of the nanoparticles and fabricated PMMA thin film which exhibiting a very brilliant colour as light strikes translating the opalescence colour of photonic crystals that exist in nature such butterflies wings and peacock feathers [29]. Morphology of every material in each stage of study was observed through scanning electron microscopy (SEM) as compiled in Figure 2. The first two images (Figure 1 (a) and (b)) show perfect ordered arrangement of fabricated PMMA in a repeated sequence of face-centered cubic (FCC) lattice structure. This structure could exhibit optical properties of photonic crystals which so called as photonic band gap (PBG) or stop band. Theoretically PBG arises as incident light strikes the structure, it will be reflected at certain wavelength relying on particles size, angle of diffraction and material refractive index according to Bragg Snell′s law.

This phenomenon enables the structure to control light according to required wavelength by modification of its size, angle or materials. Thus in this work aiming toward SERS enhancement study wavelength in range of 400 nm to 600 nm was targeted and will be discussed in details in UV-Vis spectroscopy section. Alloys NPs were examined through SEM as shown in Figure 2 (c) by drying alloy NPs solution on double tape to prevent sample loss thus from the image it could be observed that alloy NPs were actually stacked on tape. Figure 2 (d) displays the morphology of PMMA@alloy core-shell in suspension in which tiny white dots indicate alloy NPs attachment and could be seen to completely incorporates surround the PMMA sphere

In further, the percentage composition of elements especially Au and Ag in bimetallic alloy nanoparticles was analysed via energy dispersive X-rays scattering (EDS). The insert im-

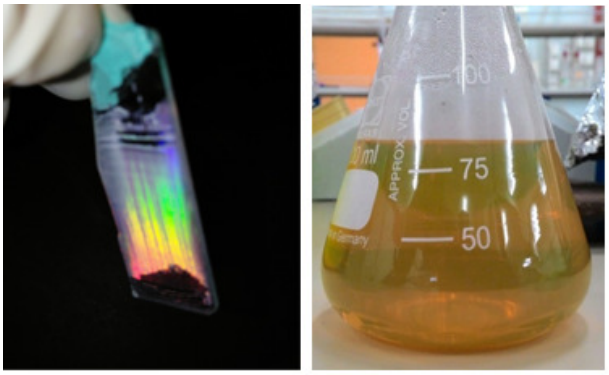

Figure 1. Photo of opalescence PMMA thin film (left) and alloy nanoparticles (right) obtained in this work.

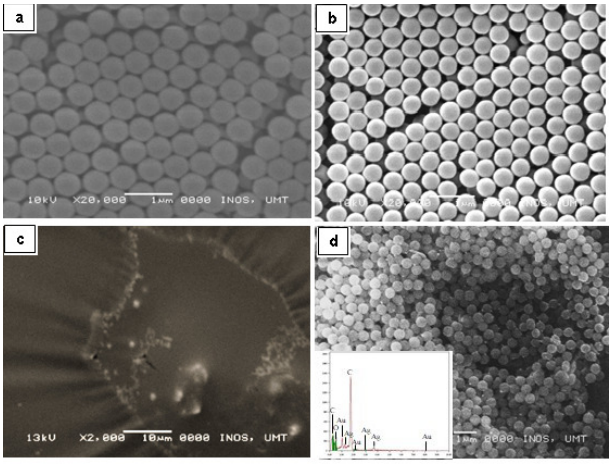

Figure 2. SEM image of a) and b) PMMA thin film, (c) alloy NPs and (d) PMMA@alloy core-shell dispersion.

age in Figure 2(d) illustrates the spectrum obtain from the EDX analysis while Table 2 summarises each element with the indicating mass percentage. 65.92 % of Au and 8.02% of Ag was analysed in alloy NPs coated 17.43% of PMMA polymer host

High percentage of Au in this bimetallic structure could be explained according to their nature of stability itself and due to strong light resistance compared to Ag. In this work we are using 1:1 ratio of Au and Ag precursor thus in order to obtained equal percentage the ratio could be tuned to 2:1 or 3:1 of Ag and Au volume

Table 2. EDS analysis for every element constituent of PMMA@alloy core-shell.

Element	(keV)	Mass %	K
C K*	0.277	17.43	9.0891
O K*		8.63	
Ag L*	2.983	8.02	8.8211
Au M*	2.121	65.92	82.0898

UV-Vis spectroscopy spectrum in Figure 3 demonstrates SPR peak of alloy NPs and PMMA@alloy core-shell at the wavelength of 451 nm and 438 nm respectively. Slight shift and less intense of PMMA@alloy core-shell as compared to alloy NPs was observed due to the assimilation of PMMA and alloy NPs dielectric environment which also contribute to the merge of SPR and the photonic band gap (PBG) properties. This SPR peak was believed could be increased by the increasing the alloy NPs composition or by decreasing polymer diameter which provides higher surface area for the incorporation sites. However for the actual usage PMMA@alloy core-shell is in thin film form thus the hybrid properties of PBG and SPR could not be study using typical UV-Vis spectroscopy. Thus Raman spectroscopy analysis will be carried out for final detection studies to confirm the applicability.

According to the findings PMMA@alloy 3D

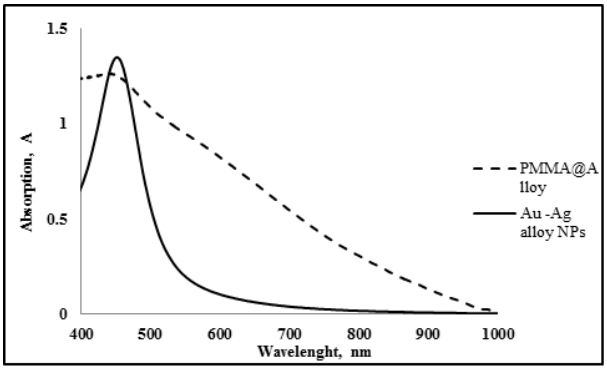

Figure 3. UV-Vis absorption spectrum of Alloy nanoparticles and PMMA@Alloy core shell.

MDPCs SERS substrate could be potentially used as SERS sensitive substrate due to its excellent plasmonic properties. Furthermore the holey structure of the core-shell particles itself have a contribution in trapping the electron and create a region of high electron density. In addition 3D MDPC SERS substrate also could be fabricated in large area and would serve large active area upon detection. Another remarkable point is it was reproducible and highly stable to be stored in long time.

IV. SUMMARY

In conclusion, the core-shell structure consist of PMMA as core and alloy (Au-Ag) as the shell was successfully synthesised in this work in developing 3D SERS substrates referring to both physical and optical properties. The core-shell advantages with interior nanogap in between Au-Ag alloy nanoparticles on the surface of PMMA sphere. Besides the fabrication of PMMA@alloy SERS substrate was performed via self-assembly method which is low cost and laboratory practise. Alloy NPs were introduced onto PMMA surface with modification using PEI. The uses of PEI successfully modified negatively charge PMMA surface to enhance the incorporation of alloy NPs. The average size of 6 nm alloy NPs was obtained with intense SPR peak at the wavelength of 438 nm indicating the improvement of plasmonic activity of alloy NPs compared to Au NPs from our previous work along with stability.

The results from the fabrication the obtained SERS substrate consisted of two properties arising from photonic crystals and metal nanoparticles that were from periodic arrangement PMMA@alloy and alloy nanoparticles respectively. These properties were so called as PBG and SPR properties each from periodic arrangement of PMMA@alloy and alloy nanoparticles enables sensitive SERS substrate. The enhancement of Raman signal was expected to gradually increased and stable for a long time period. Compared to conventional SERS substrate , the PMMA@alloy coreshell could serve the most versatile yet sensitive substrate due to the ability of alloy NPs itself in gripping SERS reporter molecule vertically possess better performance in chemical and biological analysis.

V. ACKNOWLEDGMENT

We would like to express our acknowledgement to Ministry of Higher Education Malaysia

(MOHE) for research grant FRGS 59391 and Universiti Malaysia Terengganu for research supports and facilities.

[1] Wan, F, Shi , H, Chen, W, Gu , Z, Du , L, Wang , P, Wang, J, Huang, Y, 2017, Charge Transfer Effect on Raman and Surface Enhanced Raman Spectroscopy of Furfural Molecules, *Nanomaterials*, vol. 7, pp. 1-9.

[2] Marta , S, D, Novara , C, Giorgis , F, Bonifacio, A, Sergo, V, 2017, Optimization and Characterization of Paper-Made Surface Enhanced Raman Scattering (SERS) Substrates with Au and Ag NPs for Quantitative Analysis, *Materials*, vol. 10, pp. 1-15.

[3] Lyandres, O, Yuen, M, Shah, N, C, VanDuyne, R, P, Walsh Jr, J, T, Glucksberg, M, R, 2008, Progress Toward an In Vivo Surface-Enhanced Raman Spectroscopy Glucose Sensor, Diabetes technology and therapy, vol. 10, pp. 257-265.

[4] Tian, S, Neumann, O, McClain, M, J, Yang, X, Zhou, L, Zhang, C, Nordlander, P, Halas, N, J, 2017, Aluminum Nanocrystals: a Sustainable Substrate for Quantitative SERS-based DNA Detection, *Nano Letter*, vol. 17, pp. 5071-5077.

[5] Zhu, T, Hu, Y, Yang, K, Dong, N, Yu, M, Jiang, N, 2018, A novel SERS nanoprobe based on the use of core-shell nanoparticles with embedded reporter molecule to detect E. coli O157:H7 with high sensitivity, *Microchimica Acta*, vol. 30, pp. 1-9.

[6] Gudun, K, Elemessova, Z, Khamkhash, L, Ralchenko, E, Bukasov, R, 2017, Commercial Gold Nanoparticles on Untreated Aluminum Foil: Versatile, Sensitive, and Cost-Effective SERS Substrate, *Journal of Nanomaterials*, Article ID 9182025, pp. 1-8.

[7] Tan, K, H, Tajuddin, H, A, Ahmad, R, Shuhaimi, A, Johan, M, R, 2017, Fabrications of Nanocomposite Gold-Polymer Metamaterials Consisting of Periodic Microcavities with Tunable Optical Properties Optik, vol. 150, pp. 54-61.

[8] Ghazali, N, Johan, M, R, 2016, Environmental modification of self-assembled plasmonic core-shell cluster (silica-gold nanoparticles) for surface enhanced Raman scattering (SERS), *Optical Society of America*, vol. 6, pp. 1-7.

[9] Zhang, C, Jiang, S, Z, Yang, C, Li, C, H, Huo, Y, Y, Liu, X, Y, Liu, A, H, Wei, Q, Gao, S, S, Gao, X, G, Man, B, Y, 2016, Gold@silver bimetal nanoparticles/pyramidal silicon 3D substrate with high reproducibility for high-performance SERS, *Scientific Reports*, vol. 6, pp. 1-8

[10] Perez, N, P, Puebla, R, A, 2018, *SPIE Proceedings*, vol. 10507, pp. 1-6.

[11] Kong, X, Squire, K, Wang, A, X, 2018, Fabrication of continuous and isolated 3D plasmonic micro-structured super-crystals arrays for SERS sensing, *SPIE Proceedings*, vol. 10510, pp. 1-6.

[12] Kong, X, Xi, Y, Duff , P. L, Chong, X, Li, E, Ren, F, Rorrer, G. L, Wang, A, X, 2017, Detecting explosive molecules from nanoliter solution: A new paradigm of SERS sensing on hydrophilic photonic crystal biosilica, Biosensors and Bioelectronics, vol. 88, pp. 6370.

[13] Zhao, X, Xue, J, Mu, Z, Huang, Y, Lu, M, Gu, Z, 2015, Gold nanoparticle incorporated inverse opal photonic crystal capillaries for optofluidic surface enhanced Raman spectroscopy, *Biosen-*

sors and Bioelectronics, vol. 72, pp. 268274.

[14] Gong, T, Cui, Y, Goh, D, Voon, K, K, Shum, P, P, Humbert, G, Auguste, J, L, Dinh, X, Q, Yong, K, T, Olivo, M, 2015, Highly sensitive SERS detection and quantification of sialic acid on single cell using photonic-crystal fiber with gold nanoparticles, *Biosensors and Bioelectronics*, vol. 64, pp. 227233.

[15] Mott, D, Thuy, N, T, B, Aoki, Y, Maenosono, S, 2010, Aqueous synthesis and characterization of Ag and AgAu nanoparticles: addressing challenges in size, monodispersity and structure, *Phil. Trans. R. Soc. A*, vol. 368, pp. 42754292.

[16] Verbruggen, S, W, Keulemans, M, Martens, J, A, Lenaerts, S, J, 2013, *Physical Chemistry C*, vol. 117, pp. 19142-19145.

[17] Link, S, Wang, Z, L, El-Sayed, M, A, J, 1999, Alloy Formation of GoldSilver Nanoparticles and the Dependence of the Plasmon Absorption on Their Composition, *Physical Chemistry B*, vol. 103, pp. 3529-3533.

[18] Hazra, A, Hossain, S, M, Pramanick, A, K, Ray, M, 2017, Gold-silver nanostructures: Plasmon-plasmon interaction, *Vacuum*, vol. 146, pp. 437-443.

[19] Kamaruddin , N, N, Kassim, S, Harun, N, A, 2017, Volume effect of non-polar solvent towards the synthesis of hydrophilic polymer nanoparticles prepares via inverse miniemulsion polymerization, *AIP Conference Proceedings*, 1885, 020056.

[20] Ismail, Z, Kassim, S, Harun, N, A, 2017, Development of hydrophilic poly(N-vinylpyrrolidone) nanoparticles via inverse miniemulsion polymerization technique, *AIP Conference Proceedings*, 1885, 020079.

[21] Kapeliouchko, V, Palamone, G, Poggio, T, Zuccheri, G, Passeri, R, Sparnacci, K, Antonioli, D, Deregibus, S, Laus, M, 2009, PMMAbased core-shell nanoparticles with various PTFE cores, *Journal of Polymer Science Part A: Polymer Chemistry*, vol. 47, pp. 29282937.

[22] Sa, Y, Yu, N, Wolke, J, G, C, Chanchareonsook, N, Goh, B, T, Wang, Y, Yang, F, Jansen, J, A, 2017, Bone Response to Porous Poly(methyl methacrylate) Cement Loaded with Hydroxyapatite Particles in a Rabbit Mandibular Model, Tissue Engineering: Part C, vol. 23, pp. 262-273.

[23] James, J, Thomas, G. V, Pramoda, K, P, Thomas, S, 2017, Transport behaviour of aromatic solvents through styrene butadiene rubber/poly [methyl methacrylate] (SBR/PMMMA) interpenetrating polymer network (IPN) membranes, *Polymer*, vol. 116, pp. 76-88.

[24] Totu, E, E, Nechifor, A, C, Nechifor, G, Enein, H, Y, A, Cristache, C, M, 2017, Poly(methyl methacrylate) with TiO2 nanoparticles inclusion for stereolitographic complete denture manufacturing the fututre in dental care for elderly edentulous patients?, *Journal of Dentistry*, vol. 59, pp. 68-77.

[25] Esmaeil, S, Zakiyan, Aziz, H, Ghasemi, I, 2017, *Composite Science Technology*, vol. 142, pp. 10-19.

[26] Rodriguez, E, Shahbikian, S, Marcos, B, Huneault, M, A, 2018, Hydrolytic stability of polylactide and poly(methyl methacrylate) blends, *Journal of Applied Polymer Science*, vol. 45991, pp. 1-14.

[27] Harun, N, A, Kassim, S, T /Muhammad, S, Rohi, F, E, Norzam, N, N, Tahier, N, S, M, 2017, The effect of nonionic surfactants on

emulsion polymerization of poly (methacrylic acid) nanoparticles, *AIP Conference Proceedings*, 1885 (1), 020032.

[28] Tahrin, R, A, A, Azman, N, S, Kassim, S, Harun, N, A, 2017, Preparation and properties of PMMA nanoparticles as 3 dimensional photonic crystals and its thin film via Surfactant-free emulsion polymerization, *AIP Conference Proceedings*, 1885 (1), 020092.

[29] Arora, N, Mehta, A, Mishra, A, Basu, S, 2018, 4-Nitrophenol reduction catalysed by Au-Ag bimetallic nanoparticles supported on LDH: Homogeneous vs. heterogeneous catalysis, *Applied Clay Science*, vol. 151, pp. 19